

# Modified Electrodes Using Mixed Langmuir–Blodgett Films Containing a Ruthenium Complex: Features of the Monolayers at Air–Liquid Interface

Juliane Pereira Santos, Maria Elisabete D. Zaniquelli,\* Claudemir Batalini, and Wagner Ferraresi De Giovani

Departamento de Química, Faculdade de Filosofia, Ciências e Letras de Ribeirão Preto, Universidade de São Paulo, 14040-901 Ribeirão Preto-SP, Brazil

Received: May 23, 2000; In Final Form: October 16, 2000

Mixed Langmuir–Blodgett (LB) films of arachidic acid (AA) and  $[\text{Ru}(\text{L})(\text{totpy})(\text{OH}_2)](\text{ClO}_4)_2$  ( $\text{L} = \text{Ph}_2\text{AsCH}_2\text{CH}_2\text{AsPh}_2$ ; 4-totpy = 4'-(4-tolyl-2,2':6',2''-terpyridine)) complex (2:1) were used in the preparation of modified electrodes. The incorporation of the metallic complex into mixed monolayers is noticed from the surface pressure ( $\pi$ -A) and surface potential ( $\Delta V$ -A) isotherms. The  $\pi$ -A curves show a phase transition region between the expanded and condensed liquid states (LE-LC) at 35 mN/m, which is not present in the  $\pi$ -A curves for pure AA monolayers. In the  $\Delta V$ -A isotherms there is a large expansion of the critical area and the difference between the minimum and maximum surface potential ( $\Delta\Delta V$ ) increases with the concentration of the ruthenium complex in the mixed monolayer. Combining the  $\pi$ -A curve data with the ultraviolet–visible spectra for the corresponding LB films, the dissociation degree of the fatty acid within the mixed LB films is calculated as 0.67. The FTIR spectra confirm the partial dissociation of the acid. The cyclic voltammograms of the modified electrodes of AA/ruthenium complex (2:1) at pH = 8.1, in the presence of benzyl alcohol showed pronounced enhancement of the anodic current corresponding to the  $\text{Ru}^{\text{IV}}/\text{Ru}^{\text{III}}$  couple. This is indicative of an electrocatalytic behavior.

## 1. Introduction

Aquo/oxoruthenium complexes have been studied by many research groups due to their potential application in electrocatalysis.<sup>1–4</sup> The presence of an oxo/aquo system provides fast proton and electron transfer, allowing the formation of several oxidation states. The  $\text{Ru}^{\text{IV}}$  state acts in the electrocatalytic process of several substrates:<sup>3–7</sup> alcohol, cyclic ketones, toluene, 4-picoline. The hydrophobic environment of the phosphine and arsine moieties facilitates the interaction between the  $\text{Ru}^{\text{IV}}$  catalytic site and the substrates.<sup>8</sup> The chemistry and use of oxoruthenium complexes, containing polypyridyl and tertiary phosphine ligands as oxidant, have been studied.<sup>8–10</sup>

The preparation of modified electrodes has been studied by several research groups. A large number of preparation methods is described in the literature.<sup>11–13</sup> For example, modified electrodes prepared by using polypyrrole films containing ruthenium complexes have been used in the electrooxidation of alcohols.<sup>14,15</sup> It is known that the thickness of the film and the organization of the electroactive substance influence the electrochemistry of the system.<sup>16</sup> On the other hand, thin oriented films of surfactant and sometimes nonsurfactant molecules can be provided by the Langmuir–Blodgett (LB) technique.<sup>17</sup>

LB films of ruthenium complexes<sup>18</sup> can be prepared using either modified surfactant molecules<sup>19–22</sup> or mixed monolayers<sup>23–27</sup> of an insoluble ruthenium complex with amphiphilic molecules that exhibit a large spreading coefficient and also self-spreading ruthenium copolymers.<sup>28–30</sup> In this way, mixed LB films of ruthenium aquo complex and arachidic acid can be tested as an alternative method for the preparation of modified

electrodes. However, electrocatalysis of organic substrates using ruthenium aquo complexes supported in LB films is not reported in the literature.

In this work LB films containing arachidic acid (AA) and  $[\text{Ru}(\text{L})(\text{totpy})(\text{OH}_2)](\text{ClO}_4)_2$  ( $\text{L} = \text{Ph}_2\text{AsCH}_2\text{CH}_2\text{AsPh}_2$ ; 4-totpy = 4'-(4-tolyl-2,2':6',2''-terpyridine)) complex (2:1) were characterized by UV–vis and FTIR spectroscopies, and cyclic voltammetry. The electrocatalytic properties of these modified electrodes were tested with benzyl alcohol as substrate. The behavior of the Langmuir monolayers is discussed from the surface pressure ( $\pi$ -A) and surface potential ( $\Delta V$ -A) isotherms to better understand the interaction between the ruthenium complex and the matrix provided by the oriented fatty acid molecules.

## 2. Experimental Details

**2.1. Materials.** Arachidic acid, chloroform, dichloromethane, and the reagents used in the synthesis were purchased from Aldrich Chemical Co.. Purified Milli-Q water was used in all experiments. The synthesis of  $[\text{Ru}(\text{L}(4'\text{-topty})(\text{H}_2\text{O}))](\text{ClO}_4)_2$  (complex I) was described elsewhere;<sup>31</sup> its structure is shown in Figure 1.

**2.2. Monolayers.** The liquid monolayers were prepared by the spreading of 4:1 and 2:1 mixtures of  $1.0 \times 10^{-3} \text{ mol L}^{-1}$  arachidic acid solution and  $1.0 \times 10^{-3} \text{ mol L}^{-1}$  ruthenium complex solution in chloroform on pure water subphase, at pH = 5.7. Control experiments were carried out for pure arachidic acid monolayers. The surface pressure and potential isotherms were recorded by compressing the monolayers at  $0.21 \text{ mm s}^{-1}$  ( $0.03 \text{ \AA}^2 \text{ molecule}^{-1} \text{ s}^{-1}$ ), after allowing a period for solvent evaporation (ca. 20 min).

\* To whom correspondence should be addressed. E-mail: medzaniquelli@ffclrp.usp.br.

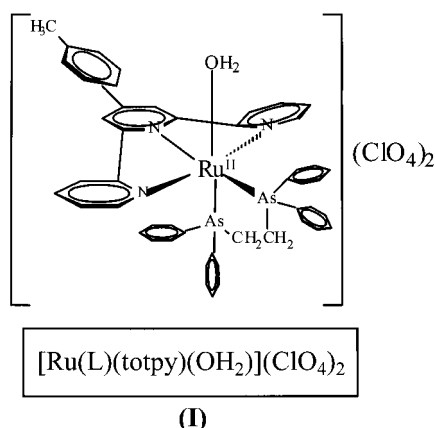


**Figure 1.** Structure of  $\text{Ru}[\text{L}(4'-\text{totpy})(\text{H}_2\text{O})](\text{ClO}_4)_2$  ( $\text{L} = (\text{C}_6\text{H}_5)_2\text{AsCH}_2\text{CH}_2\text{As}(\text{C}_6\text{H}_5)_2$ ; 4-totpy = 4'-(4-tolyl-2,2':6',2''-terpyridine)).

**2.3. LB Film Preparation.** After the  $\pi$ -A isotherms have been recorded, the monolayers were submitted to expansion-compression cycles, before keeping the surface pressure at  $25 \pm 0.5 \text{ mN m}^{-1}$ . Silanized quartz plates, glassy carbon electrodes, and zinc selenide windows were used as solid substrates according to the technique employed to analyze the films. The deposition rate was  $0.03 \text{ mm s}^{-1}$ . The depositions, up to 25 monolayers on silanized quartz and zinc selenide, were "X" type and 2–8 monolayers on glassy carbon electrode were "Z" type.

**2.4. Electrochemical Measurements.** The cyclic voltammograms were performed in a one-compartment cylindrical electrochemical cell using, as the working electrode, a glassy carbon plate electrode ( $1 \text{ cm}^2$ ) modified by layers of the mixed film; a Pt wire as the counter electrode and a saturated calomel reference electrode (SCE), in phosphate buffer solution (pH 8.1). The bulk electrolysis experiments were performed in a two-compartment cylindrical electrochemical cell using the ruthenium LB film modified glassy carbon plate electrode as the working electrode, a platinum plate auxiliary electrode and SCE ( $25 \pm 1^\circ\text{C}$ ). The electrolyses were performed at a fixed applied potential of 1.00 V which is sufficient to generate the  $\text{Ru}^{\text{IV}}=\text{O}^{2+}$  oxidant from the corresponding  $\text{Ru}^{\text{II}}-\text{OH}_2^{2+}$  complex.

**2.5. Instruments.** The Langmuir films were studied on a  $459.40 \text{ cm}^2$  homemade Langmuir trough and the surface pressure was measured using the Wilhelmy plate technique, hanging a filter paper from a Cahn C-32 microbalance. The surface potential measurements were carried out in a Faraday cage using a radioactive  $\text{Am}^{143}$  electrode (5 mm distant from the surface) and a SCE located into the subphase. The electrodes were connected to a Keithley 617 Programmable electrometer. All these instruments were interfaced to a computer.

The electronic spectra were recorded on a UV-vis Hitachi U-3000 spectrophotometer. The FTIR spectra were obtained from a Nicolet 5ZDX spectrophotometer, in the transmission mode, using 100 scans at  $4 \text{ cm}^{-1}$  resolution.

The electrochemical experiments were carried out with an EG&G model 273A galvanostat-potentiostat.

### 3. Results and Discussion

**3.1. Interaction between Ruthenium Complex I and the Fatty Acid at the Air-Liquid Interface.** The ruthenium complex I is insoluble in water and it was co-spread with the fatty acid. Figure 2 shows that the presence of different concentrations of the ruthenium complex in the arachidic acid monolayer induces changes on the  $\pi$ -A curve transitions. The collapse features and the minimum area per molecule are also

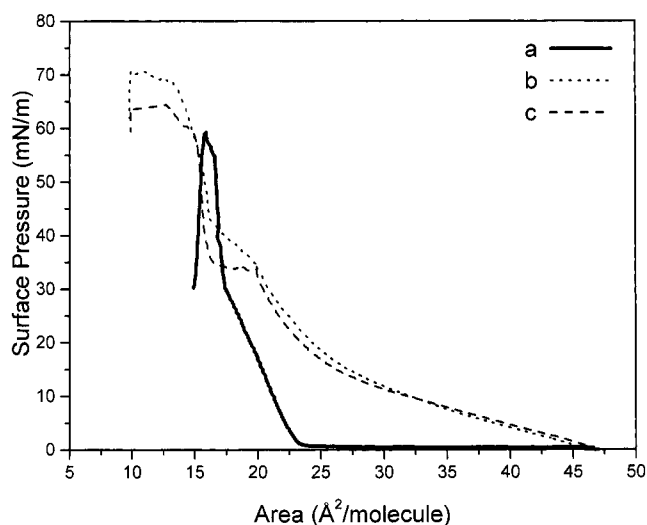


**Figure 2.**  $\pi$ -A isotherms for arachidic acid monolayer (a) and a mixed monolayer of arachidic acid/complex I (4:1) (b) and (2:1) (c) on pure water (pH = 5.7).

modified. The  $\pi$ -A curves for mixed monolayers of AA/ruthenium complex I using 4:2 and 2:1 ratios are presented in the Figure 2b,c, respectively. For the mixed monolayers, it is possible to observe an expanded liquid state at large areas and a LE-LC transition region that is not present in the isotherms for pure AA monolayers (Figure 2a). The transition for the mixed monolayer, using the 2:1 ratio, is about  $35 \text{ mN/m}$  and it is almost parallel to the abscissa axis, characteristic of pure substance transition. In this case, the mixture 2:1 resembles the tridimensional eutectic mixture, suggesting some miscibility of the ruthenium complex with the fatty acid molecules at the liquid-air interface. On the other hand, this effect is also analogous to that produced by simple rising the subphase pH for pure arachidic acid monolayer.<sup>32</sup> On pure water (pH = 5.7) almost all the carboxylic groups of arachidic acid molecules do not dissociate and it is reported the existence of a "crystalline" monolayer. By increasing the pH to approximately 12, for instance, a plateau region is observed in a surface pressure ranging from 11 to  $15 \text{ mN m}^{-1}$ , which is much lower than the one reported in this paper for the mixed monolayers. The plateau region has been attributed, in the case of ionized pure arachidic acid monolayer, to the consumption of compressional energy for the conformational change of the alkyl chain. Thus, for the system reported in this work, the presence of the ruthenium complex I increases the packing energy for the hydrophobic chains of the fatty acid molecules. This packing is responsible for driving the monolayer to the condensed state. The chains, being less condensed in the presence of the complex, should work as a better matrix.

Increasing the dilution, as in the mixed monolayer of AA/ruthenium complex I (4:1), the LE-LC transition is shifted to higher surface pressure and the plateau region is no longer observed. Once the ruthenium complex is electrically charged, the dilution within the monolayer would correspond to the decreasing of electrolyte concentration in the study of the influence of ions (like sodium) on the electrostatic interaction in phospholipid monolayers.<sup>33</sup> In this sense, the effect here observed resembles more that observed for monolayers formed in the presence of divalent ions, which can coordinate the headgroups, causing the hydrophobic chains approximation. For larger compressions, the minimum area per molecule for the mixed monolayers in both proportions (4:1) and (2:1) are roughly similar to the minimum area for pure AA monolayer.

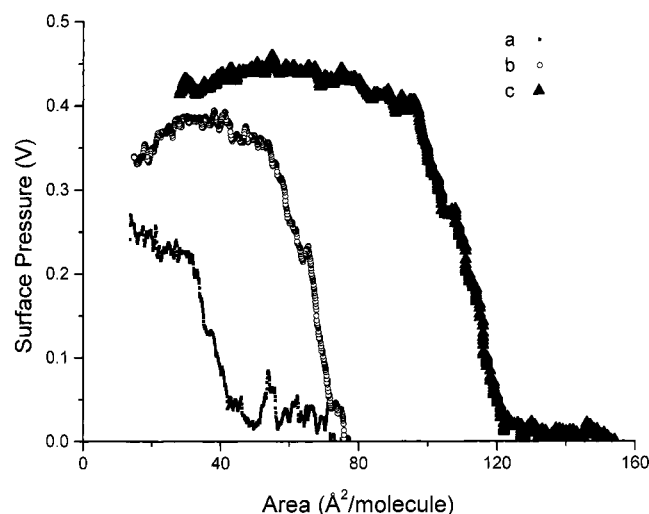


**Figure 3.**  $\Delta V$ - $A$  isotherms for arachidic acid monolayer (a) and a mixed monolayer of arachidic acid/complex I (4:1) (b) and (2:1) (c) on pure water (pH = 5.7).

**TABLE 1: Features for the Surface Potential Isotherms**

monolayer	$A_c$ ( $\pm 1$ ) ( $\text{\AA}^2/\text{molecule}$ )	$\Delta\Delta V$ ( $\pm 10$ ) (mV)
AA	40	250
AA/complex I (4:1)	78	370
AA/complex I (2:1)	120	430

These results indicate that the Ru complex is expelled from the air-liquid interface, remaining underneath the monolayer binding to the polar headgroups of the fatty acid, at surface pressure higher than 35 mN/m for the 2:1 proportion and above 38 mN/m for 4:1 AA/complex I ratio.

Therefore, from the  $\pi$ - $A$  curves data and the corresponding interpretation given above, we can conclude that the miscibility of the two components mixed monolayer is due to some specific interaction between the complex and the fatty acid headgroups, inducing packing modification of the fatty acid alkyl chains.

The surface potential curves for AA, AA/complex I (4:1), and AA/complex I (2:1) monolayers are showed in Figure 3a-c. The areas for which the surface potential suddenly increase, or critical areas,<sup>34</sup> and the difference between the minimum and the maximum surface potential,  $\Delta\Delta V$ , are resumed in Table 1.

Yazdanian and Hyuk<sup>35</sup> showed that divalent ions as magnesium, calcium, and barium, which interact electrostatically with fatty acid molecules, cause an increase in the surface potential of liquid monolayers as the concentration of these ions in the subphase is increased. However, divalent ions as cadmium, cobalt, and lead, which exhibit predominant covalent interaction, induce a decrease in the surface potential. It was also reported that the different type and concentration of ions within the subphase influence the ionization of the headgroup of the compound forming the monolayer.

Shapovalov and Tronin<sup>36</sup> also describe the effects on the surface potential caused by hydrophobic ions interacting with Langmuir monolayers. The effect of the least hydrophobic ion is less pronounced and the ion adsorbs to the headgroup; the more hydrophobic ones affect considerably the surface potential and the ions are in fact incorporated to the monolayer. In this sense the hydrophobic character of the complex I, with arsine groups, should be responsible for the large differences in the surface potential curves. Also, this should be the cause for the presence of the complex at the interface until high surface

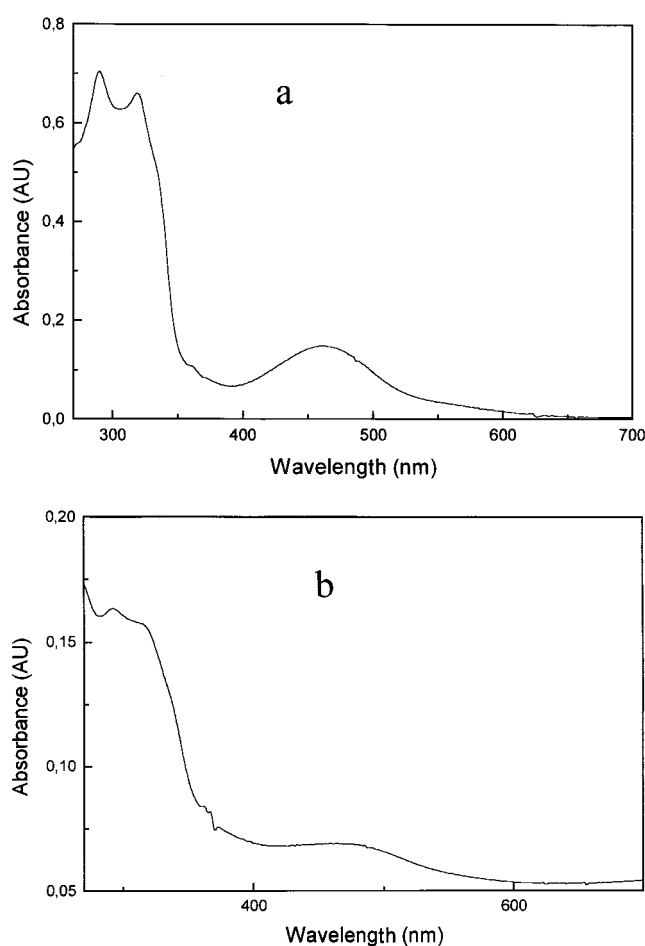


**Figure 4.** Absorption spectra for  $1.0 \times 10^{-4} \text{ mol L}^{-1}$  complex solution I in chloroform (a) and a mixed LB film of arachidic acid/complex I (2:1) deposited on a hydrophobic quartz plate (25 layers each side) (b).

pressures (35–38 mN/m). This is in accordance to our finding<sup>26</sup> in previous work for a ruthenium complex with phosphine ligand, less hydrophobic than arsine, because the surface potential curves are only slightly modified compared to the pure fatty acid curve and in this case the complex remains underneath the monolayer, even at low surface pressures. These data, together with the  $\pi$ - $A$  curves, indicate that the interaction between AA and the ruthenium complex I is not predominantly ionic pair as the one observed in our previous work.

**3.2. Mixed LB Films from Arachidic Acid and Ru Complex I.** From the analysis presented above we chose to prepare LB films from the 2:1 (AA:complex I) mixed monolayers, considering that one could have a better miscibility of the fatty acid and the ruthenium complex. The films were transferred at  $25 \text{ mN m}^{-1}$ , lower than the expulsion surface pressure for the complex.

The electronic spectrum of 25 layers of AA/ruthenium complex I mixed LB films deposited on silanized quartz (Figure 4b) resembles that obtained for the ruthenium complex in solution (Figure 4a). A broad band at 300 nm is attributed to  $\pi \rightarrow \pi^*$  transitions of the ligand and a band at 470 nm to the metal-ligand charge transfer.<sup>37</sup> Using the molar extinction coefficient ( $5800 \text{ mol}^{-1} \text{ dm}^3 \text{ cm}^{-1}$  at 470 nm) for the complex in solution<sup>31</sup> and the absorbance for the LB film, it is possible to attain a surface concentration per layer of  $1.45 \times 10^{14} \text{ molecules cm}^{-2}$  for the ruthenium complex in the LB film. The surface density at the air-liquid interface, calculated from the  $\pi$ - $A$  curve, is  $4.65 \times 10^{14} \text{ molecules cm}^{-2}$  for arachidic acid.

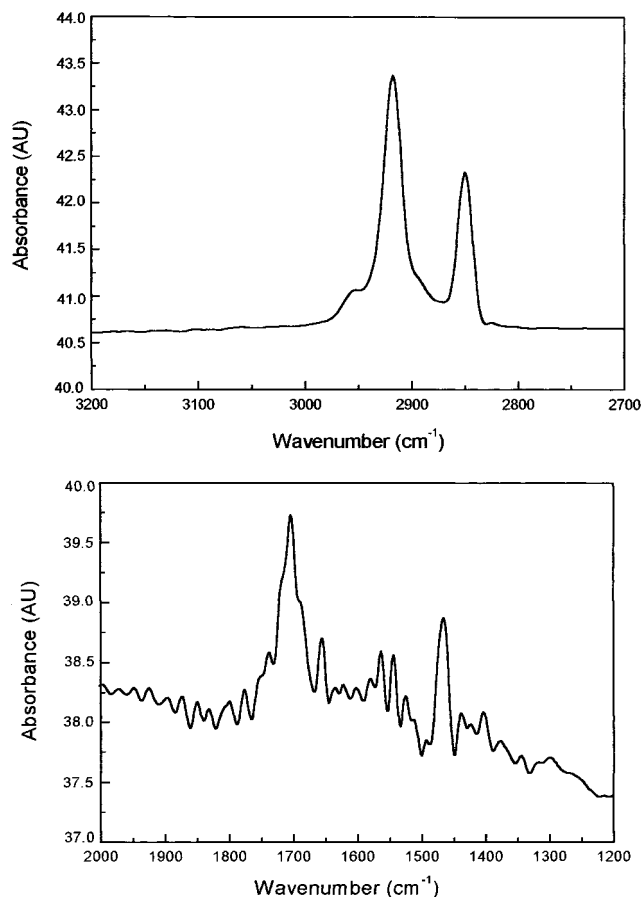


**Figure 5.** FTIR absorption spectra for a mixed LB film of arachidic acid/complex I (2:1) deposited on zinc selenide plate (25 layers each side).

This number could indicate a stoichiometry within the LB film of 3:1 arachidic acid/ruthenium complex. However, this value differs from that used for preparing the liquid monolayers, 2:1.

FTIR spectrum (Figure 5) of 25 monolayers of mixed LB films deposited on zinc selenide shows the asymmetric and symmetric methylene stretching from the C18 alkyl chain of AA at 2925 and 2850  $\text{cm}^{-1}$ , respectively. The  $\text{CH}_2$  bending vibrations of the aliphatic chains appear as a singlet at 1465  $\text{cm}^{-1}$ . Generally, the occurrence of this band as a singlet is interpreted<sup>38,39</sup> as a triclinic packing symmetry, where all molecular planes are parallel to one another, which is not expected from the surface pressure we have used for the deposition in this work. Therefore, this criterion should be used cautiously. The strong  $\text{C}=\text{O}$  stretching at 1700  $\text{cm}^{-1}$ <sup>40</sup> is characteristic of the development of dimer species of carboxylic acid by H-bonding and is a proof of incomplete dissociation of the fatty acid. The asymmetric and symmetric  $\text{COO}^-$  stretching vibrations that appear at 1540 and 1392  $\text{cm}^{-1}$  are attributed to the carboxylate groups. The presence of both carboxylate and dimer carboxylic acid bands indicates that the monolayer is partially ionized. It confirms that the electrostatic interaction is not dominant within the film as we have already deduced from the  $\pi$ -A and  $\Delta V$  curves. The other bands that appear in the spectrum are due to  $\nu_s$  C-C from the ligands, pyridine and phenyl rings in the complex I being distributed in the 1615–1415  $\text{cm}^{-1}$  region.

As we could attest by the FTIR data, the ionization is only partial. Then, we associate the UV-vis spectrum and the surface pressure data to evaluate the dissociation degree ( $\alpha$ ) of the arachidic acid within the LB mixed films; its value is 0.67.

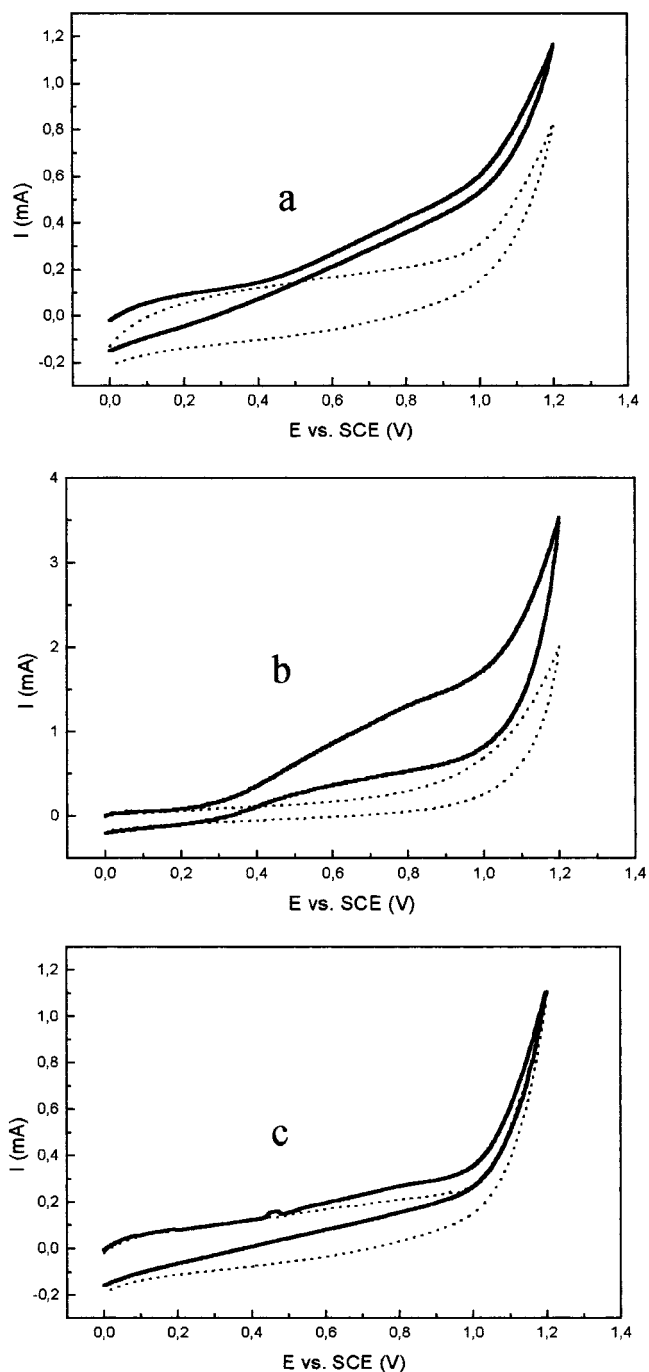


**Figure 6.** Cyclic voltammograms using modified electrodes of arachidic acid/complex I (1:2) coated on glassy carbon electrode, depositing 2 (a), 5 (b), and 8 layers (c) in the presence of benzyl alcohol (—) and without benzyl alcohol (---). Conditions: pH = 8.1, phosphate buffer solution, scan rate of 50 mV/s.

**3.3. Electrocatalytic Activity of the Modified LB–Ru Complex Electrodes.** The cyclic voltammograms of the C/AA/ruthenium complex I modified electrode (2:1) at pH = 8.1 phosphate buffer in the presence of benzyl alcohol show a substantial catalytic anodic current at +0.8 V, corresponding to the couple  $\text{Ru(III)/Ru(IV)}$  (Figure 6). The cyclic voltammograms of the modified electrodes in the absence of benzyl alcohol do not show oxidation peaks at +0.34 and +0.77 V, observed for this complex in solution<sup>31</sup> at the same pH.

The influence of the number of deposited layers on the modified electrodes shows that there is an optimum condition for electrodes prepared depositing 5 monolayers (Figure 6b). For these modified electrodes it is possible to observe an



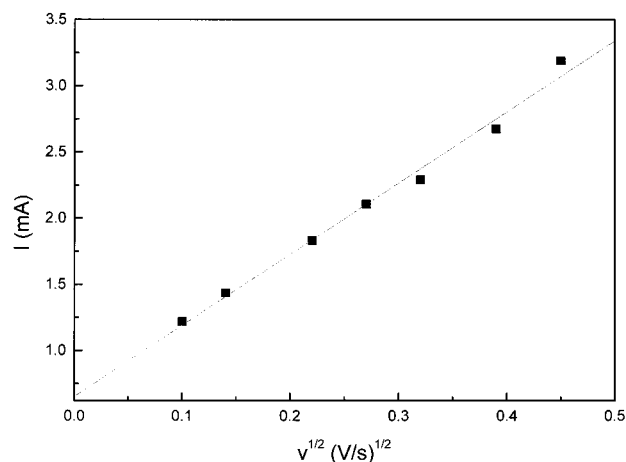


**Figure 7.** Plot of the oxidation peak currents against square root of the potential scan rate of a C/AA/complex I (2:1) modified electrode in 50 mmol L<sup>-1</sup> benzyl alcohol solution at pH = 8.1.

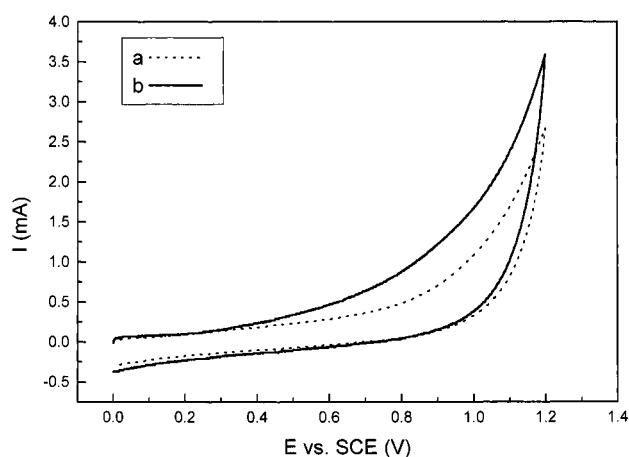


**Figure 8.** Cyclic voltammogram for five layers of arachidic acid/complex I (2:1) coated on a glassy carbon electrode at pH = 8.1, phosphate buffer solution and scan rate of 50 mV/s, before (a) and after (b) benzyl alcohol electrooxidation.

increase in the current, displaying a peak at about +0.8 V. In this way, these electrodes show a better catalytic response than the electrodes prepared from 2 (Figure 6a) or 8 (Figure 6c) layers.

For quantitative evaluation of the surface electrocatalysis,<sup>41</sup> the dependence of the peak height on the scan rate was studied. Figure 7 shows that the dependence of the peak height on the square root of the potential scan rate for concentration of 50 mmol L<sup>-1</sup> in the range 20–100 mV s<sup>-1</sup> is linearly correlated. This behavior is characteristic of surface electrocatalysis with a catalyst confined to the electrode surface under diffusional rate control of the substrate from the bulk solution.<sup>41</sup>

Figure 8 shows the cyclic voltammograms obtained for the modified electrode in electrolyte solution before (curve 8a) and after (curve 8b) the electrode be used in the electrooxidation of benzyl alcohol. The current at curve 8b is higher than that displayed in curve 8a. This feature indicates that some adsorption process is occurring at the electrode surface. The electrolyses of benzyl alcohol using the modified electrode shown an initial very fast decrease in the current that was stabilized after 30 min. However, the time required for the complete benzyl alcohol oxidation, using the same concentration of this substrate, in homogeneous catalysis is about 6 h. This fast current decrease can be attributed to irreversible adsorption of the original organic substrate, intermediates or the final oxidation products on the

modified electrode surface that was also attested by cyclic voltammetry (Figure 8).<sup>42,43</sup>

#### 4. Conclusion

This paper shows that a matrix that is usually thought as solid as arachidic acid at low pH, and with low possibility for dissolving solutes, can render a fluid behavior even at relatively low areas in terms of the acid depending on the co-spreading material. Electrocatalysis of the organic substrate, benzyl alcohol, was accomplished using the ruthenium complex modified electrodes. Nevertheless, diffusional processes and adsorption of the organic substrates or intermediates need to be solved to improve the system.

**Acknowledgment.** The authors would like to express their gratitude for the financial support received from CNPq/PADCT, FAPESP, and CAPES.

#### References and Notes

- (1) Oliveira, S. M.; De Giovanni, W. F.; Miller, J.; Romero, J. R. *J. Braz. Chem. Soc.* **1992**, *3*, 70.
- (2) Takeuchi, K. J.; Thompson, M. S.; Pipes, D. W.; Meyer, T. J. *Inorg. Chem.* **1984**, *23*, 1845.
- (3) Thompson, M. S.; De Giovanni, W. F.; Moyer, B. A.; Meyer, T. J. *J. Org. Chem.* **1984**, *49*, 4972.
- (4) Carrijo, R. M.; Romero, J. R. *Synth. Commun.* **1994**, *24*, 433.
- (5) Navarro, M.; De Giovanni, W. F.; Romero, J. R. *Synth. Commun.* **1990**, *20*, 399.
- (6) De Giovanni, W. F.; Deronzier, A. *J. Electroanal. Chem.* **1992**, *337*, 285.
- (7) Meyer, T. J. *J. Electrochem. Soc.* **1984**, *131*, 221C.
- (8) Marmion, M. E.; Takeuchi, K. J. *J. Chem. Soc., Dalton Trans.* **1988**, *9*, 2385.
- (9) Muller, J. G.; Acquaye, J. H.; Takeuchi, K. J. *Inorg. Chem.* **1992**, *31*, 4552.
- (10) Marmion, M. E.; Takeuchi, K. J. *J. Am. Chem. Soc.* **1988**, *110*, 1472.
- (11) Watkins, B. F.; Behling, J. R.; Kariv, E.; Miller, L. L. *J. Am. Chem. Soc.* **1975**, *97*, 3549.
- (12) Deronzier, A.; Moutet, J. C. *Coord. Chem. Rev.* **1996**, *147*, 339.
- (13) Moses, P. R.; Murray, R. W. *J. Am. Chem. Soc.* **1976**, *98*, 7435.
- (14) De Giovanni, W. F.; Deronzier, A. *J. Chem. Soc., Chem. Commun.* **1992**, *19*, 1461.
- (15) Sauthier, M. N. C. D.; Deronzier, A.; LeBozec, H.; Navarro, M. *J. Electroanal. Chem.* **1996**, *410*, 21.
- (16) Goldenberg, L. M. *J. Electroanal. Chem.* **1994**, *379*, 3.
- (17) Gaines, G. L., Jr. *Insoluble Monolayers at Liquid-Gas Interface*; Interscience: New York, 1966.
- (18) Guérin, F.; Tian, Y.; Fendler, J. H. *J. Phys. Chem. B* **1999**, *103*, 7882.
- (19) Valenty, S. J.; Behnken, D. E.; Gaines, G. L., Jr. *Inorg. Chem.* **1979**, *18*, 2160.
- (20) Zhang, X.; Bard, A. J. *J. Phys. Chem.* **1988**, *92*, 5566.
- (21) Zhang, X.; Bard, A. J. *J. Am. Chem. Soc.* **1989**, *111*, 8098.
- (22) Fu, Y.; Ouyang, J.; Lever, A. B. P. *J. Phys. Chem.* **1993**, *97*, 13753.
- (23) Fujihira, M.; Yanagisawa, M.; Kondo, T.; Suga, K. *Thin Solid Films* **1992**, *210/211*, 265.
- (24) DeArmond, A. H.; Dvorak, O.; DeArmond, M. K. *Thin Solid Films* **1993**, *232*, 115.
- (25) Murakata, T.; Miyashita, T.; Matsuda, M. *J. Phys. Chem.* **1988**, *92*, 6040.
- (26) Santos, J. P.; Batalini, C.; Zaniquelli, M. E. D.; De Giovanni, W. F. *Thin Solid Films* **1999**, *349*, 238.
- (27) Samba, H.; DeArmond, M. K. *Langmuir* **1994**, *10*, 4157.
- (28) Aoki, A.; Miyashita, T. *Chem. Lett.* **1996**, *7*, 534.
- (29) Taniguchi, T.; Fukasawa, Y.; Miyashita, T. *J. Phys. Chem. B* **1999**, *103*, 1920.
- (30) Aoki, A.; Miyashita, T. *J. Electroanal. Chem.* **1999**, *473*, 125.
- (31) Batalini, C. Ph.D. Thesis, University of São Paulo, 1998.
- (32) Oishi, Y.; Yoshinari, T.; Suehiro, K.; Kajiyama, T. *Langmuir* **1997**, *13*, 2527.
- (33) Helm, C. A.; Laxhuber, L.; Lösche, M.; Möhwald, H. *Colloid Polym. Sci.* **1986**, *264*, 46.
- (34) Oliveira, O. N., Jr.; Taylor, D. M.; Lewis, T. J.; Salvagano, S.; Stirling, C. J. M. *J. Chem. Soc., Faraday Trans. 1* **1989**, *85*, 1009.

- (35) Yazdanian, M.; Hyuk, Y.; Zografi, G. *Langmuir* **1990**, *6*, 1093.
- (36) Shapovalov, V.; Tronin, A. *Langmuir* **1997**, *13*, 4870.
- (37) Durham, B.; Wilson, S. R.; Hodgson, D. J.; Meyer, T. J. *J. Am. Chem. Soc.* **1980**, *102*, 600.
- (38) Peltonen, J. P. K.; Lindén, P. H. M.; Rosenholm, J. B. *J. Phys. Chem.* **1994**, *98*, 12403.
- (39) Lindén, M.; Rosenholm, J. B. *Langmuir* **1995**, *11*, 4499.
- (40) Dhanabalan, A.; Talwar, S. S.; Major, S. S. *Thin Solid Films* **1997**, *298*, 237.
- (41) Lima, E. C.; Fenga, P. G.; Romero, J. R.; De Giovanni, W. F. *Polyhedron* **1998**, *17*, 313.
- (42) Andrade, A. R.; Donate, P. M. C.; Alves, P. P. D.; Fidellis, C. H. V. *J. Electrochem. Soc.* **1998**, *145*, 3839.
- (43) Richer, J.; Lipkowitz, J. *J. Electrochem. Soc.* **1986**, *133*, 121.